JOURNAL OF SOLID STATE CHEMISTRY **122,** 74–80 (1996)
ARTICLE NO. 0084

Mechanisms of Incipient Chemical Reaction between $Ca(OH)_2$ and SiO_2 under Moderate Mechanical Stressing

I: A Solid State Acid–Base Reaction and Charge Transfer Due to Complex Formation

Tomoyuki Watanabe, Tetsuhiko Isobe, and Mamoru Senna[1]

Faculty of Science and Technology, Keio University, 3-14-1 Hiyoshi, Yokohama 223, Japan

Received August 28, 1995; accepted November 9, 1995

Mechanisms of an incipient reaction between $Ca(OH)_2$ and SiO_2 under mechanical stressing are studied mainly by detailed infrared (IR), X-ray photoelectron (XPS), and solid state ^{1}H-NMR spectroscopies. Pretreatments by H–D exchange, adsorption of pyridine or ammonia were carried out prior to IR spectroscopy. From the comparison between the separate and mixed-milling, a solid state acid–base reaction and simultaneous dehydration are revealed. Subsequent charge transfer, confirmed by XPS, leads to the formation of a precursor of complex oxides involving Ca–O–Si bonding. © 1996 Academic Press, Inc.

1. INTRODUCTION

Solid state mechanochemical processes are often considered as a method of synthesis of complex oxides. Problems discouraging the practical application are, among others, contamination from machinery parts and high energy consumption. To surmount these drawbacks, rapid reaction systems should be chosen, where hydroxyl groups are contained at least in one of the reaction ingredients. We have been developing such systems under the concept of soft mechanochemistry (1).

Mechanochemical synthesis from systems containing water was already reported in some detail by Avvakumov and his co-workers (2). They found a number of reactions taking place more rapidly than those between simple oxides, even against the expectation from thermodynamic data (2, 3). For a rapid solid state mechanochemical reaction, hydroxyl groups on the solid surface play an important role (1–5). Water generated by mechanical dehydration can serve as a solvent for the reactants, or induce hydrothermal effects (2, 6). On top of that, active sites produced by *in situ* mechanical dehydration interact with each other (5). Hydroxyl groups on the surface behave as acidic or basic sites, particularly when they are combined with reduced coordination numbers of surface cations or anions (7, 8).

In our previous report (5), we found that the number of basic sites on the surface of $Ca(OH)_2$ rapidly increases on milling. The basicity increases even more rapidly with a maximum when milled together with SiO_2. The manner of the change in the basicity is closely related with the solid state acid–base reaction.

In the present study, we discuss the changes of the surface hydroxyl groups, including coordination numbers of $-$OH, and of acidity due to mechanochemical activation in the $Ca(OH)_2$–SiO_2 system, by using adsorption of ammonia or pyridine as probe gas molecules, coupled with thorough infrared and solid state ^{1}H-NMR studies, partly with a preliminary H–D exchange. Furthermore, the charge transfer, being the result of the acid–base interaction, is discussed on the basis of X-ray photoelectron spectroscopy (XPS).

2. EXPERIMENTAL

A commercial reagent (Wako, guaranteed grade, 99.9%) was used as a source of $Ca(OH)_2$. The specific surface area was 7.19 $m^2 \cdot g^{-1}$, as determined by the BET method with N_2 adsorption. As a SiO_2 source, fumed silica powder (Degussa, Aerosil 200) was used. One gram of sample was milled in air batchwise with varying milling time by using a laboratory sized vibration mill (Glen-Creston), with an amplitude of 50 mm and a frequency of 12 Hz. Eight nylon coated iron balls, 9.8 mm in diameter, and a cylindrical PTFE container (26.1 cm^3) were used.

Infrared spectroscopy was carried out for the determination of the local structure of the surface OH groups by substituting a part of the surface OH groups with OD groups by the H–D exchange operation, in order to distinguish the surface OH from those in the bulk. FT-IR measurement was carried out by using a self-support disk method (9) (BIO-RAD, FTS 175). Surface acidic sites were

[1] To whom all correspondence should be addressed.

0022-4596/96 $18.00

characterized by NH_3 (Nihon Sanso : 99.999%) and pyridine (Wako : 99.5%) adsorption followed by IR spectroscopy. Since ^{1}H-NMR is a versatile tool for the purpose of direct characterization of the nature of surface hydroxyl groups, we carried out NMR analyses by using a high resolution solid state unit (Chemagnetics Inc. CMX-300) with the method combined rotation and multiple pulse (CRAMPS) NMR spectroscopy.

The charge transfer at the mechanically activated interface between $Ca(OH)_2$–SiO_2 was examined by X-ray photoelectron spectroscopy (XPS, JEOL JPS-90SX) which enables us to reveal the O 1*s*, Ca 2*p*, and Si 2*p* electronic states of oxides. The binding energy of Au $4f_{7/2}$ was used as a standard to calibrate the effect of charge up. To estimate the thickness of the reacted layer in the mixed-milled samples, we used 500 V Ar ion etching, the ion current density, 1 mA · cm^{-2}. Under this condition, the erosion rate of the flat silica glass was confirmed to be 0.72 nm · sec^{-1} by an atomic force microscope (AFM, SEIKO Instruments Inc. SPA300).

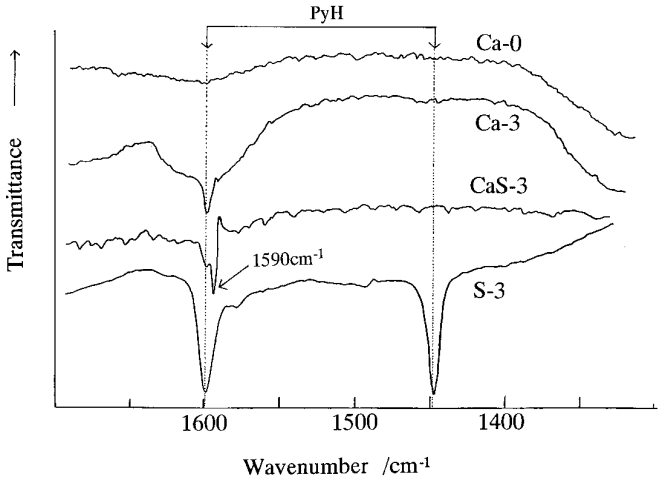

FIG. 1. Differential IR spectra of pyridine adsorbed Ca-0 (initial $Ca(OH)_2$), Ca-3($Ca(OH)_2$ milled separately for 3 h), CaS-3 (mixed-milling for 3 h), and S-3 (SiO_2 milled separately for 3 h). The assignments are shown by connected lines (see Ref. (9–11)).

3. RESULTS AND DISCUSSION

3.1. Measurements of Change in the Acidic Sites Due to Milling by Molecules Probes

Pyridine is frequently used as a probe molecule to examine the properties of the surface acidic sites, since it chemisorbs selectively by its lone paired electrons bound to the nitrogen on the specific points where the local surface electron density is low. Three modes of adsorption, hydrogen bond type (PyH), Lewis acidic type (PyL) and Brønsted acidic type (PyB), are well established (9–11).

Differential IR spectra, i.e., those between after and before pyridine adsorption, are shown in Fig. 1. The following changes are appreciable after the adsorption. First of all, milling silica alone (S-3) brought about absorption bands typical for the PyH bond due to surface silanol, as marked by arrows in Fig. 1. These bands due to surface silanol drastically decreased on milling in the presence of $Ca(OH)_2$ (see CaS-3). The reduction of the band due to PyH is attributed to the donation of silanolic protons from the silica surface to the basic site of the hydroxyl groups of $Ca(OH)_2$, resulting in the mechanochemical dehydration. This tallies well with the loss of OH groups from $Ca(OH)_2$ on mixed milling, as reported previously (5).

A new distinct absorption band is observed at 1590 cm^{-1} in CaS-3 after pyridine adsorption. This new band must be associated with a new, stronger PyH acidic site formed by an acid–base solid state reaction at the silica/$Ca(OH)_2$ interface under mechanical stressing. On milling $Ca(OH)_2$ alone (Ca-3), PyH band appeared at 1600 cm^{-1} along with broad wings extending between 1530 and 1670 cm^{-1}. This PyH adsorption corresponds to the increase in the acidity as a result of reduced oxygen coordination number around cations and consequent stronger acceptors of the electron. These changes are related with an on-top type of hydroxyl groups (cf. Ref. (12) Fig. 3(1)–(3)), with a broad distribution of oxygen coordination number, like a hollow site type shown in Ref. (12). Since these sites are consumed as base during the mechanochemical acid–base reaction between $Ca(OH)_2$ and SiO_2, no broad band is observed for CaS-3. In the case of milling $Ca(OH)_2$ alone, the bands due to other modes of pyridine adsorption at around 1450 cm^{-1} were absent. This indicates that acidic sites formed on separately milled $Ca(OH)_2$ are not strong enough to induce PyL or PyB type adsorption.

Although pyridine adsorption is well-defined, it is not very suitable for the examination of dissociative adsorption on the juxtaposed acid–base pair sites. Pyridine is also inconvenient for the sample with micropores because of its relatively large molecular diameter. An alternative IR spectroscopy was, therefore, carried out by using NH_3 as a probe, in order further to examine the properties of surface acid species imparted with milling. Figures 2 and 3 show differential spectra, just after NH_3 adsorption and after evacuation at 1.3×10^{-3} Pa, respectively. The latter was carried out for the purpose of forced desorption.

The former peak at 1097 cm^{-1} and a shoulder at 1600 cm^{-1} are observed for the separately milled $Ca(OH)_2$, as shown in Fig. 2. They are attributed to the coordination of ammonia due to the entrapped unpaired electron by Ca^{2+} with the low coordination number Lewis acidic site (13). They are absent on the mixed-milled sample, CaS-3. A prominent peak at 1472 cm^{-1} is observed only on the separately milled SiO_2 and not on the mixed-milled one. This is attributed to the formation of ammonium ions,

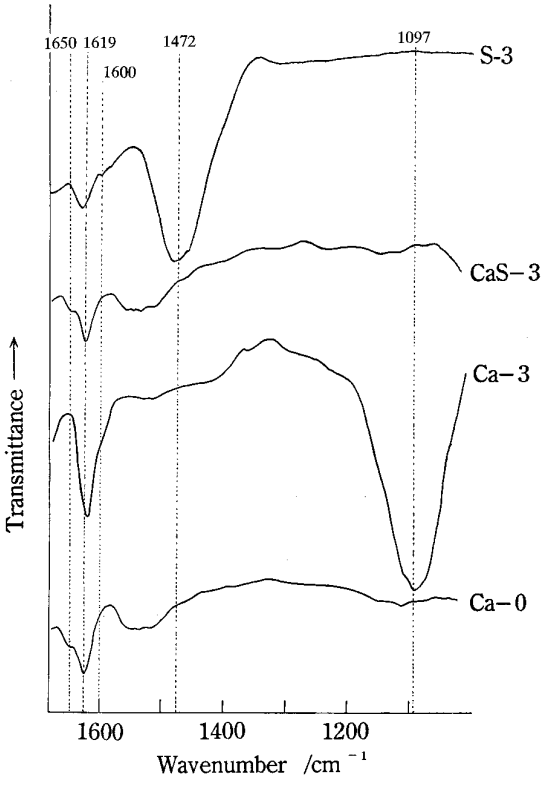

FIG. 2. Differential IR spectra of ammonia adsorbed Ca-0, Ca-3, CaS-3, and S-3 at 173 Pa.

formed by a proton transfer from a surface silanol, Si–OH (14).

On the other hand, ammonia adsorption on intact $Ca(OH)_2$ (Ca-0) and the mixed-milled sample (CaS-3) shows a doublet absorption bands, whose larger and smaller peaks are located at 1619 and 1650 cm^{-1}, respectively. The first is attributed to the hydrogen bond adsorption of NH_3 on the surface hydroxyl groups of $Ca(OH)_2$ by lone-paired nitrogen electrons of NH_3 (13). As a result of the formation of surface basic sites, –OH and O^{2-}, juxtaposed by a surface hydrogen atom of hydroxyl groups and available for hydrogen bond adsorption, a part of the hydrogen bond adsorption peak must have shifted from 1619 to 1650 cm^{-1} (13). This is also observed on intact $Ca(OH)_2$ since ammonia as a probe molecule is capable of adsorption on the weaker acidic sites compared with pyridine.

There is close relation between the above-mentioned two observations; i.e., Lewis acidic sites, Ca^{2+}, are found only on the separately milled $Ca(OH)_2$, Ca-3, and the common existence of the band at 1650 cm^{-1} on the intact $Ca(OH)_2$, as well as on the mixed-milled sample, CaS-3. On separate milling of $Ca(OH)_2$, mechanochemical dehydration is only possible by disproportionation of two initially identical hydroxyl groups into a neutral water molecule, leaving an O^{2-} ion. The latter anion serves as a basic site, while the Ca^{2+} bound with O^{2+} serves as a Lewis acidic site. This is compatible with the present IR observation as well as what we have discussed in our previous study by temperature programmed desorption (TPD) (5). This further explains the absence of the band due to Lewis acidic site after mixed-milling, because of the consumption of these sites by the reaction with silica to form Si–O–Ca bonds. Survival of the band at 1650 cm^{-1} on the mixed-milled sample (CaS-3) is explained simply by the nature of the stronger acidity of silanolic OH as compared with a hydroxyl group of Ca–OH. This parallels with the disappearance of the band at 1472 cm^{-1} due to the silanolic Brønsted site on mixed-milling.

On evacuation, all the bands due to NH_3 adsorption on the surface acidic sites decreased significantly, as shown in Fig. 3, as a consequence of forced desorption. On a closer look, however, the relative extent of decrease in the intensity was different between the two bands at 1619 and 1650 cm^{-1}. The intensity of the IR band of 1619 cm^{-1} relative to that at 1650 cm^{-1} becomes larger for both Ca-0 and CaS-3 on evacuation, as revealed by comparing Fig. 3 with Fig. 2. This indicates the stronger coordination of NH_3 when the surface O^{2-} base site is highly polarized as a result of a hydrogen bond with NH_3.

On the sample Ca-3, a weak absorption at around 1583 cm^{-1}, once overwhelmed by the large band at 1472 cm^{-1}

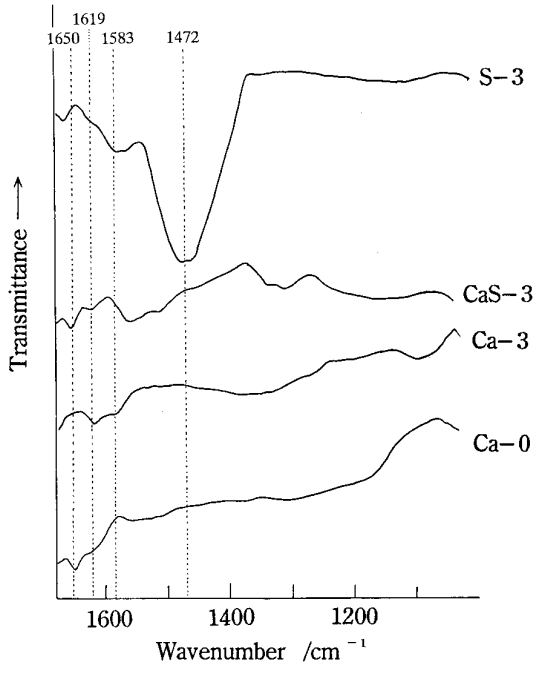

FIG. 3. Differential IR spectra of ammonia adsorbed Ca-0, Ca-3, CaS-3, and S-3 after outgassing at room temperature for 60 min to reduce the pressure to 10^{-3} Pa for the purpose of forced desorption.

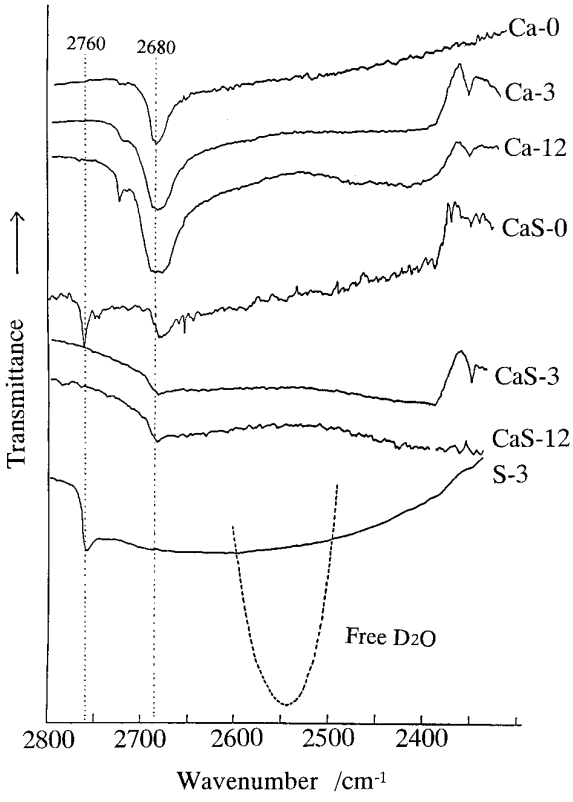

FIG. 4. Changes of O–D vibrational IR absorption bands of milled samples. The dotted line at the bottom denotes the vibrational band for the free D_2O molecule.

before evacuation, becomes detectable. This small peak is attributed to the deformation of NH_2^-[i], as a result of dissociation, $NH_3 + O^{2-} \rightarrow NH_2^- + OH^-$ (13–15), at the moment of adsorption. In contrast, no sign of NH_2^-, i.e., dissociative adsorption of NH_3, was detected on the mixed-milled sample. Consumption of Ca^{2+}–O^{2-} pair sites disables dissociative adsorption to form NH_2^-. Consumption of the pair sites is only explained by the Ca–O–Si bond formation.

3.2. Characterization of Surface Hydroxyl Groups by D_2O Probe Adsorption

IR spectra of milled samples after the exchange a part of hydrogen atoms on the surface hydroxyl groups with deuterium atoms are shown in Fig. 4. In the case of milling $Ca(OH)_2$ alone, a remarkable absorption band due to the O–D stretching vibration is observed at about 2680 cm^{-1}, however, on milling a mixture of $Ca(OH)_2$ and SiO_2 the absorption band at about 2680 cm^{-1} decreases. This indicates the reduction of OD groups as a result of mechanochemical dehydration, by mixed-milling, as already reported elsewhere (5), where the decrease of the surface basic sites of the hydroxyl groups by mixed-milling was discussed.

A band, being assigned as silanolic –OD, at around 2760 cm^{-1} is observed on the surface of milled silica without the presence of calcium hydroxide (sample S-3) and a physical mixture, CaS-0. This band completely disappears on milling a mixture (CaS-3). This also shows consumption of silanol, again, suggesting the reaction with strong basic sites of $Ca(OH)_2$, giving rise to the precursor of calcium silicates. This is compatible with the disappearance of the silanolic acidic site on mixed-milling, as mentioned in Section 3.1. This contrasts with the result of separate milling. On the intact $Ca(OH)_2$ (sample Ca-0), only a band corresponding to fully coordinated Ca is observed at around 2680 cm^{-1}. On milling calcium hydroxide alone, the absorption band grew and broadened toward a lower wave number (see samples Ca-3 and Ca-12 in Fig. 4).

The change in the peak profile on milling can be attributed to two factors. The first is a decrease of the anion coordination number from 6 to 5 or 4. This induces polarization of O–D, since a decrease in the oxygen coordination number leads to the decrease in the electron density around a calcium atom, and hence, increases the relative contribution of the electrons bound to the oxygen of O–D groups, weakening the O–D bonds. This, in turn, facilitates the formation of surface oxygen ion, imparted to the mechanochemical dehydration. This tallies well with the reported increase in the surface basicity (5), since mechanochemical dehydration induces the formation of O^{2-}, serving as surface basic sites.

The second factor, being a consequence of the foregoing, is a bidentate, dissociative readsorption of D_2O on the juxtaposed acid–base sites on the less coordinate cations and anions. This mechanism accords with the idea suggested by Stone *et al.* (16, 17), i.e., dissociative adsorption is promoted by the decrease of the anion and cation coordination number. They also report that the dissociative adsorption of H_2O occurs more easily than that of NH_3. Knowing that the dissociative adsorption of NH_3 was observed on the separately milled $Ca(OH)_2$, dissociative adsorption of D_2O must also have taken place on the sample Ca-3.

A very broad band, also observed between 2400 and 2550 cm^{-1} on samples Ca-3 and Ca-12, is likely to be attributed to the hollow site –OD(12) adsorption. The formation of hollow site type OD groups can be explained by dissociative adsorption of D_2O either preexisted in the milling milieu or formed by mechanochemical dehydration. This broad band is not observed on the mixed-milled sample. Therefore, it is also conceivable from the viewpoint of dissociative adsorption after disproportionation, that juxtaposed acid–base sites formed by milling were immediately consumed through the formation of a Si–O–Ca complex.

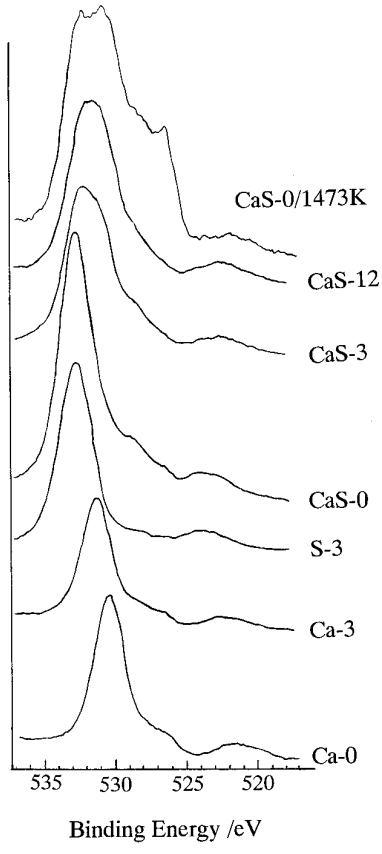

FIG. 5. X-ray photoelectron spectra of O 1*s*; for separately milled samples (Ca-*t*) and mixed-milled samples (CaS-*t*), where -*t* indicates the milling time in hours. The profile of calcium silicate, obtained by firing the $Ca(OH)_2$–SiO mixture at 1473 K, is also shown on the top of the figure.

3.3. Charge Transfer at $Ca(OH)_2$–SiO_2 Interface

Charge transfer during milling is visualized by the chemical shifts of XPS, shown in Figs. 5 to 7 for O 1*s*, Ca 2*p*, and Si 2*p* electrons, respectively. Assignments of respective peaks are given in Table 1. On intact and separately milled $Ca(OH)_2$, the O 1*s* peak from Ca–OH at 530 eV is predominant. A slight shift toward the high energy side on milling is attributed to the weakening of the Ca–OH bonds from that of the structural ones to that of adsorbed water. This tallies well with the appearance of –OH basic sites on milling (5). The XPS spectra from the sample S-0 were not shown, simply because they were quite similar to those from CaS-0 and S-3. The similarity of the O 1*s* bands observed between CaS-0 and S-3 might be attributed to the eventual coating of the $Ca(OH)_2$ surface by ultrafine silica particles.

As asymmetric peak shape of CaS-3 and CaS-12 with tailing toward the lower energy side, similar to the profile of calcium silicate (CaS-0/1473 K), suggests a chemical interaction between SiO_2 and $Ca(OH)_2$. The chemical interaction is most likely achieved by the migration or short-range diffusion of Ca^{2+} due to mechanical stressing, and a consequent microscopic flow into the near-surface region of silica to form Ca–O–Si bonding.

The change due to mixed-milling is more remarkable for Ca 2*p* electron binding energy. As shown in Fig. 6, the peak at 346 eV for Ca–O increased remarkably against that for Ca–OH at 350 eV, on milling with SiO_2. This is not the case on separate milling. This tallies well with the remarkable increase in the surface basicity on mixed milling, as reported previously (5). It is to be noted that the shape of Ca 2*p* peaks for CaS-3 is similar to that of CaS-0/1473 K. The Ca 2*p* XPS profile of sample CaS-3 turns back to that of CaS-0 on sputtering by Ar^+ only for 1 or 2 sec (see CaS-3/E1 and /E2, respectively). Therefore, the thickness of the layer of interaction is proved to be localized at the outermost layer, less than 1.5 nm, of the mixed-milled sample.

The change in the Si 2*p* on milling is even more remarkable. As shown in Fig. 7, a signal from Si^{2+} at 101 eV, being only a shoulder on the physical mixture before milling, CaS-0, becomes by far the predominant on mixed-milling for 3 h (CaS-3). Since no such increase in Si^{2+} is observed on separate milling (S-3), reduction of Si^{4+} to

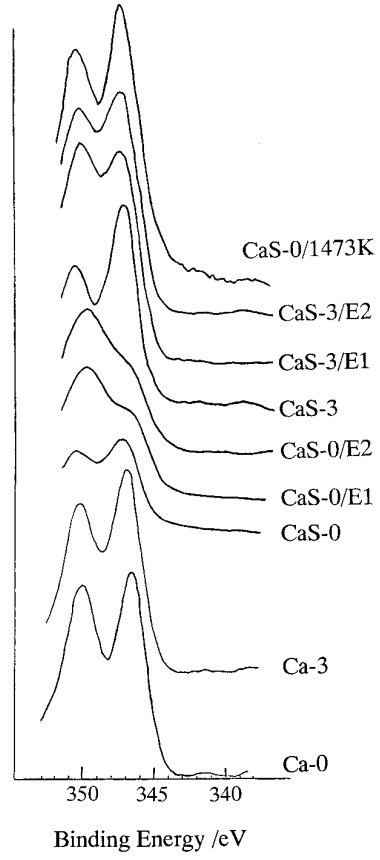

FIG. 6. X-ray photoelectron spectra of Ca 2*p*; for separately milled samples (Ca-*t*) and mixed-milled samples (CaS-*t*), where -*t* indicates the milling time in hours and /*E* shows the Ar ion etching time in seconds.

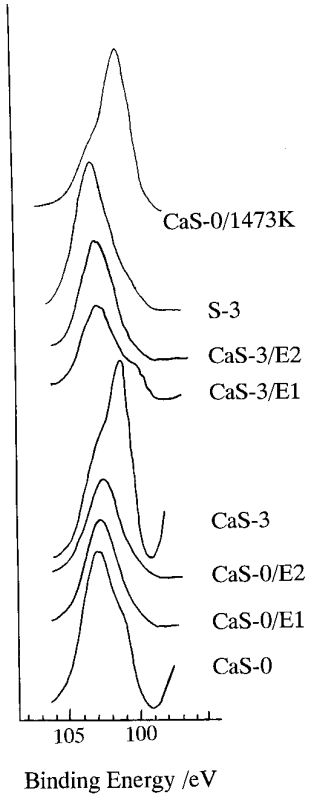

FIG. 7. X-ray photoelectron spectra of Si 2*p*; separately milled sample (Ca-*t*) and mixed-milled samples (CaS-*t*), where -*t* indicate the milling time in hours and /*E* shows the Ar ion etching time in seconds.

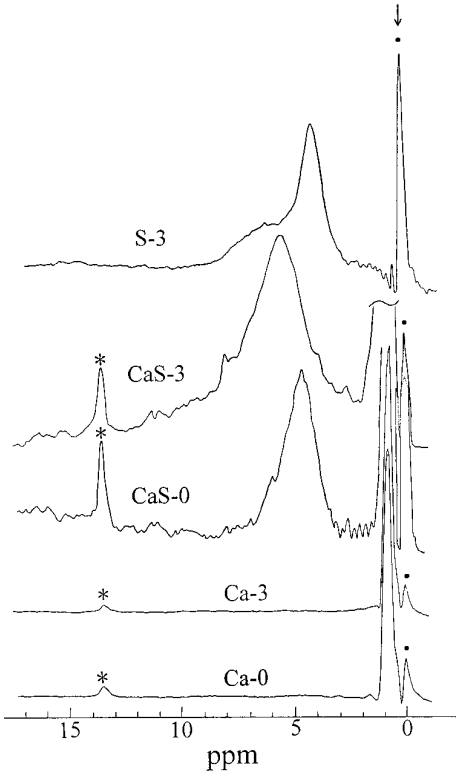

FIG. 8. ^{1}H-CRAMPS-NMR spectra of the initial $Ca(OH)_2$ (Ca-0), milled for 3 h (Ca-3), SiO_2 milled for 3 h (S-3), and the mixtures $Ca(OH)_2$–SiO_2, before milling (CaS-0), and milling for 3 h (CaS-3), where * denotes the spinning side band of $Ca(OH)_2$. A common peak at 0.12 ppm, marked by an arrow, represents a signal from a silicon rubber used as a standard.

Si^{2+} is necessarily be attributed to the mechanochemical reaction with $Ca(OH)_2$, and not to the simple Si–O bond breakage. This is explained briefly by the electron transfer from oxygen to silicon due to higher electronegativity of Si, as a consequence of proton transfer and, hence, formation of Ca–O–Si bonds after mechanochemical dehydration. Such a chemical shift, accompanied by the formation of Ca–O–Si, is observed on calcium silicate prepared by heating CaS-0 to 1473 K. Similar reduction of the cation due to reactive charge transfer is observed by the sputtering of Ag and Pt on SiO_2 (20), as well as by the mechanical alloying of Al with TiO_2H_2O (21).

The strong signal from Si^{2+} disappeared again on Ar^+ etching for 2 sec, indicating again, that the reaction layer is not more than 1.5 nm. Thus, mechanically induced diffusion of cationic species on milling is restricted to the order of a single nanometer as far as the $Ca(OH)_2$–SiO_2 system is concerned.

TABLE 1
Binding Energies of O 1*s*, Ca 2*p*, and Si 2*p*

	Binding energy (eV)	Assignment	Literature
O 1*s*	533	SiO_2 lattice	(18)
	530	OH, H_2O, CO_2	(19)
	528	$Ca(OH)_2$ lattice	(19)
Ca 2*p*	350	Ca–OH	(19)
	346	Ca–O	(19)
Si 2*p*	103	Si^{4+}	(18, 20)
	101	Si^{2+}	(18, 20)

3.4. Change in the Chemical States of Proton Examined by ^{1}H-NMR

^{1}H-CRAMPS-NMR profiles are shown in Fig. 8 for the samples Ca-0, Ca-3, CaS-0, CaS-3, and S-3. In all the profiles containing $Ca(OH)_2$, the peak due to bulk –OH of $Ca(OH)_2$ at 1 ppm is observed, together with the spinning side band at 13.5 ppm. No remarkable changes are observed on milling $Ca(OH)_2$ alone, because of the large abundance of bulk hydroxyl groups. A small peak at 5 ppm is observed only on the mixed samples and S-3, and is attributed to the silanolic proton (22). This peak shifts

toward higher frequency on mixed milling. On milling silica alone, a broad peak appears at 6–8 ppm, apart from that at 5 ppm. The former peak is likely to be attributed to the stronger acidic sites on the surface of silica, appearing as a result of the decrease in the coordination number of Si.

A much larger and sharper peak appears at 6 ppm on mixed-milling. According to Brunner *et al.* (23), there is an inverse proportionality between the NMR chemical shift and the IR absorption wave number. Peri further suggests that the smaller wave number of IR absorption due to surface hydroxyl reflects the higher acidity (7, 8). It is, therefore, to be concluded that the new peak appeared on separate milling of silica at higher frequency demonstrates the formation of a new Si-containing species with higher acidity. The formation of the new acidic site is due to a decrease of the coordination number of OH around Si and hence, increased polarization of –OH. Such a decrease in the coordination number is obviously attributed to the partial amorphization of the silica surface, by the mechanism similar to the dangling bond formation on milling quartz (24, 25).

On the mixed-milled sample, CaS-3, the absence of the broad peak for stronger acidic sites is obviously attributed to the consumption of polarized OH, bound to less coordinated Si atoms in conjunction with mechanochemical dehydration. The strong peak at 6 ppm is presumably related to the partial reduction of Si^{4+} to Si^{2+}, as already mentioned in Section 3.3, i.e., the formation of Ca–O–Si, as well as a decrease of the coordination number of OH around Si.

4. CONCLUSION

Rapid solid state mechanochemical reactions between oxides in the presence of hydroxyl groups are initiated by the mechanochemical dehydration and resulted in acid–base sites. This induces charge transfer, i.e., proton and electron transfer, leading to a precursor of complex oxides involving Ca–O–Si bonding.

ACKNOWLEDGMENT

The authors thank Mr. Sugisawa in JEOL Ltd., for CRAMPS measurements.

REFERENCES

1. M. Senna, *Solid State Ionics* **63–65,** 3 (1993).
2. E. G. Avvakumov, *Chem. Sustainable Dev.* **2,** 1 (1994).
3. E. G. Avvakumov, E. T. Devyatkina, and N. V. Kosova, *J. Solid State Chem.* **113,** 379 (1994).
4. J. Liao and M. Senna, *Thermochimica Acta* **210,** 89 (1992).
5. T. Watanabe, J. Liao, and M. Senna, *J. Solid State Chem.* **115,** 390 (1995).
6. R. Kiriyama, Y. Tamai, and F. Kanamaru, *Nippon Kagaku Zasshi* **88,** 618 (1967).
7. J. B. Peri, *J. Phys. Chem.* **69,** 211 (1965).
8. J. B. Peri, *J. Phys. Chem.* **69,** 220 (1965).
9. E. P. Parry, *J. Catal.* **2,** 371 (1963).
10. R. B. Borade, A. Adnot, and S. Kaliaguine, *J. Chem. Soc. Faraday Trans.* **86,** 3949 (1990).
11. M. R. Carrot, P. Carrot, M. Brotas, and K. W. S. Sing, *J. Chem. Soc. Faraday Trans.* **89,** 579 (1993).
12. T. Shido, K. Asakura, and Y. Iwata, *J. Chem. Soc. Faraday Trans. 1* **85,** 441 (1989).
13. S. Couccia, S. Lavagnino, and L. Marchese, *J. Chem. Soc. Faraday Trans. 1* **85,** 477 (1987).
14. Y. Shen, S. L. Suib, M. Deeba, and G. S. Koermer, *J. Catal.* **146,** 483 (1994).
15. R. Echterhoff and E. Knozinger, *Surf. Sci.* **230,** 237 (1990).
16. F. S. Stone, E. Garrone, and A. Zecchina, *Mater. Chem. Phys.* **13,** 331 (1985).
17. A. Zecchina, M. G. Lofthouse, and F. S. Stone, *J. Chem. Soc. Faraday Trans. 1* **71,** 1476 (1975).
18. E. Paparazzo, M. Fanfoni, and E. Severini, *Appl. Surf. Sci.* **56–58,** 866 (1992).
19. Y. Inoue and I. Yasumori, *Bull. Chem. Soc. Jpn.* **54,** 1505 (1981).
20. T. Shimaguchi and M. Komiyama, *Shokubai* **34,** 104 (1992).
21. Y. Kojima, T. Isobe, M. Senna, T. Shinohara, S. Ono, K. Sumiyama, and K. Suzuki, *J. Mater. Res.* in press.
22. C. E. Bronnimann, R. C. Zeigler, and G. E. Maciel, *J. Am. Chem. Soc.* **110,** 2023 (1988).
23. E. Brunner, H. G. Karge, and H. Pfeifer, *Z. Phys. Chem.* **176,** 173 (1992).
24. T. Fukuchi, *Appl. Radiat. Isot.* **44,** 179 (1993).
25. U. Steinike, U. Kretzschmar, I. Ebert, H. P. Henning, L. I. Barsova, and T. K. Jurik, *React. Solids* **4,** 1 (1987).